

SPRING24 +20TH GCPS

A Joint AIChE and CCPS Meeting

NATECH SCENARIO ANALYSIS: OIL SPILLS TRIGGERED BY THE IMPACT OF EXTREME HYDROLOGICAL PHENOMENA ON STORAGE TANKS

JULIO ALFONSO DEL VASTO URUEÑA
*Bachelor of Water Resources Engineering and
Environmental Management. M.Sc. (candidate)*
SACS Consultores
Bogotá D.C., Colombia
Julio.delvasto@sacsconsultores.com

CAROLINA LÓPEZ PÉREZ
Chemical Engineer Esp.
SACS Consultores Bogotá
D.C., Colombia
director.consultoria@sacsconsultores.com

Prepared for Presentation at
American Institute of Chemical Engineers
2024 Spring Meeting and 20th Global Congress on Process Safety
New Orleans, LA
March 24-28, 2024

AIChE shall not be responsible for statements or opinions contained
in papers or printed in its publications

NATECH SCENARIO ANALYSIS: OIL SPILLS TRIGGERED BY THE IMPACT OF EXTREME HYDROLOGICAL PHENOMENA ON STORAGE TANKS

JULIO ALFONSO DEL VASTO URUEÑA¹

*Bachelor of Water Resources Engineering and
Environmental Management. M.Sc. (candidate)*

SACS Consultores

Bogotá D.C., Colombia

Julio.delvasto@sacsconsultores.com

CAROLINA LÓPEZ PÉREZ

Chemical Engineer Esp.

SACS Consultores Bogotá

D.C., Colombia

director.consultoria@sacsconsultores.com

Keywords: Flood, technological risk, hydrocarbon storage tank, oil spill, NaTech, computational spill simulation.

Abstract

The increasing industrialization brings with it an increase in the handling of hazardous substances (toxic and ecotoxic) and the occupation of new areas for the placement of facilities, whose location is often chosen without considering exposure to natural threats, thus creating a technological risk scenario in which, as a consequence of the occurrence of a natural event on the infrastructure, harmful agents can be accidentally released into public health and the environment, events known as NaTech (technological accidents triggered by natural events - Natural disasters triggering TECHnological accidents).

The design and operation of equipment, processes, structures, and oil facilities follow a set of international industry standards and norms that, in terms of safety, are designed to withstand operational or internal process forces (temperature, pressure, flow rate, flows, etc.), without considering the action of external forces (Cozzani et al., 2009), such as those exerted by velocity (shear forces) and water depth during flooding events.

Thus, the present work aims to analyze the force exerted by an extreme hydrological event on an industrial installation, specifically on a vertical petroleum storage tank; the mode or type of vessel failure and the consequences resulting from the loss of hydrocarbon containment (LOC), using two-dimensional modeling techniques to analyze the flooding, spill behavior, and pool fire generated by the spill.

1 Overview of NaTech Risk

The increasing industrialization brings with it an increase in the storage and handling of hazardous substances and the occupation of new areas for the placement of facilities, whose

location is often selected without taking into account exposure to natural threats, thus configuring a technological risk scenario, in which as a consequence of the manifestation of a natural event on industrial infrastructure, harmful agents for public health and the environment can be accidentally released, events known under the term NaTech (technological accidents triggered by events of natural origin - Natural disasters triggering TECHnological accidents), (Cruz et al., 2004; Showalter & Myers, 1994).

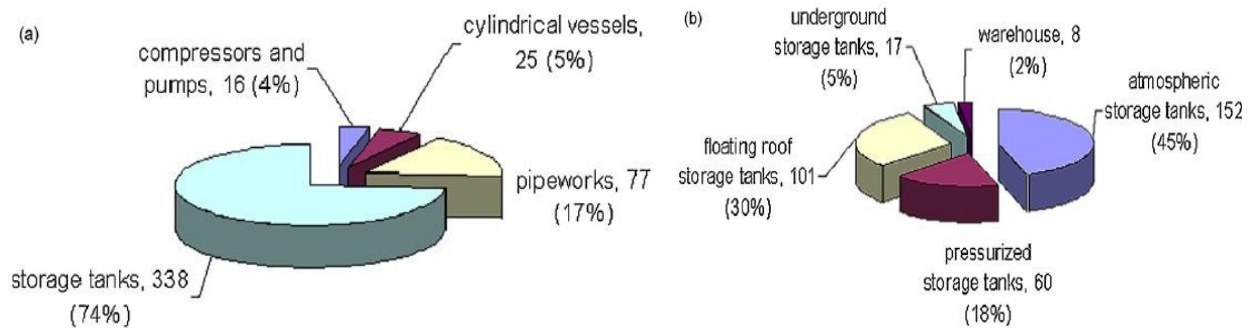


Image 1. Categories of equipment mainly involved in accidents caused by floods: (a) general categories; (b) detail of storage tanks. Source: V. Cozzani et al., 2010.

Aspects such as industrialization, population growth, community densification, and climate change have led to an increase in the frequency and severity of NaTech events (Krausmann et al., 2017), with the serious consequences they bring, as seen in the catastrophic events in Kocaeli, Turkey (1999), Tohoku, Japan (2011), Ventanilla, Peru (2022), and Canton Quijos, Ecuador (2023), among others. These events demonstrate, in general terms, the fragility of processes, equipment, and facilities in the face of external forces (Di Maio, F et al., 2022). On the other hand, there are legislations for adapting to climate change with technical gaps in the risk management regulations surrounding NaTech events, which hinder institutional capacity and governance (Pilone, E. et al., 2022).

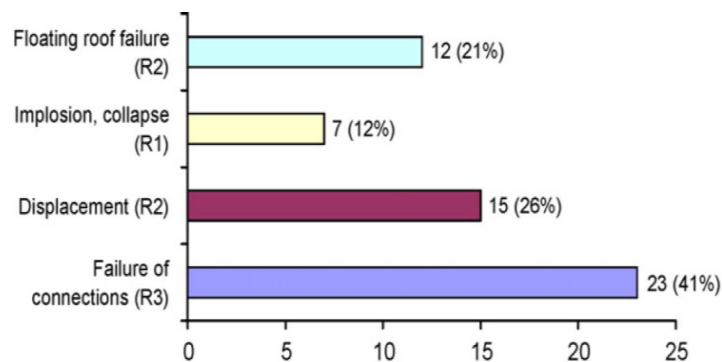


Image 2. Data available on the types of structural damage experienced by process equipment during floods and the associated release category. Results obtained from the analysis of 57 events. Source: V. Cozzani et al., 2010.

The phase and hazardousness of the substance involved in the Loss of Containment (LOC) in a NaTech event depend on the process, equipment, and installation affected by the natural phenomenon. The severity of the event in terms of quantity released, dispersion, and affected receptors depends on the type of natural phenomenon triggering the accidental loss of containment, with floods, thunderstorms, and earthquakes being the main initiators of these incidents (Krausmann et al., 2008). In this regard, the oil infrastructure, as a high-risk industry (Yanting & Liyun, 2011), whose location or placement in the global context covers vast areas of territory, is exposed to different natural threats, with hydrocarbon storage tanks being the most affected equipment (V. Cozzani et al., 2010) and with greater criticality

due to the high inventories of oil that could potentially be spilled in such an event (Image 1).

Among the main damages or effects suffered by this type of equipment due to floods, according to Campedel, 2009, are structural damage (displacements, impacts with floating objects, collapse) and electrical failures in the sensors that automate the associated processes (image 2), while the most serious consequences are those related to the dispersion and chemical reaction of the hazardous substance in water (Image 3).

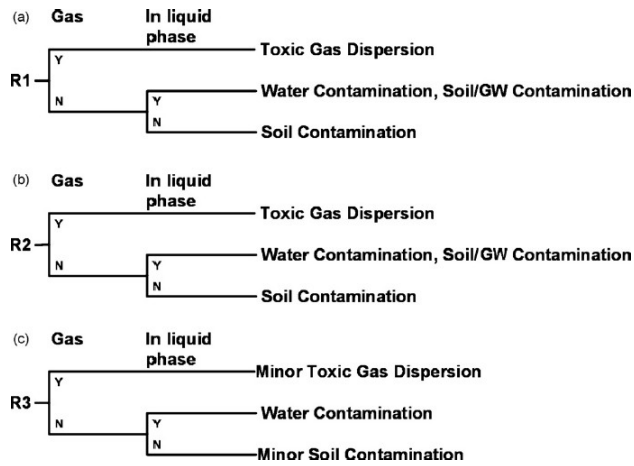


Image 3. Event trees following the release of toxic substances in NaTech accidents caused by floods. (a) Spill category R1; (b) Spill category R2; (c) Spill category R3. Source: V. Cozzani et al., 2010.

According to U.C. Lovain (2023), since the 1970s, there has been a significant increase in the occurrence of natural events worldwide, with increases of over 500% compared to 2022 (image no. 4). In the specific case of extreme hydrological events (image no. 5), the increase reaches over 400% compared to the same year, figures that are closely correlated with the occurrence of NaTech events, according to Ricci et al., 2022 (image no. 6).

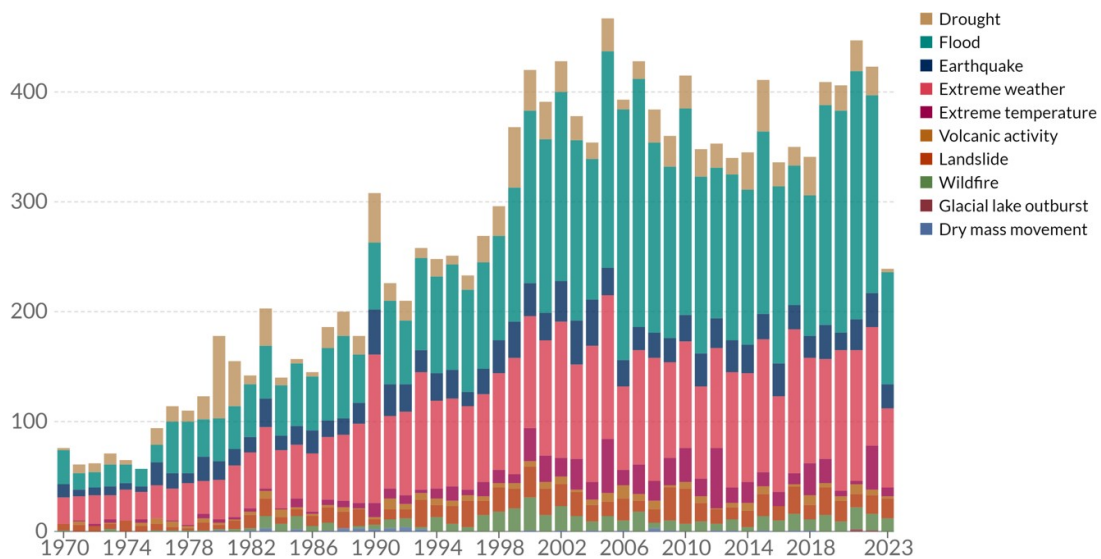


Image 4. – Global report of natural disasters by type between 1970 and 2023. Source: EM-DAT, CRED / UCLouvain (2023). <https://ourworldindata.org/natural-disasters>

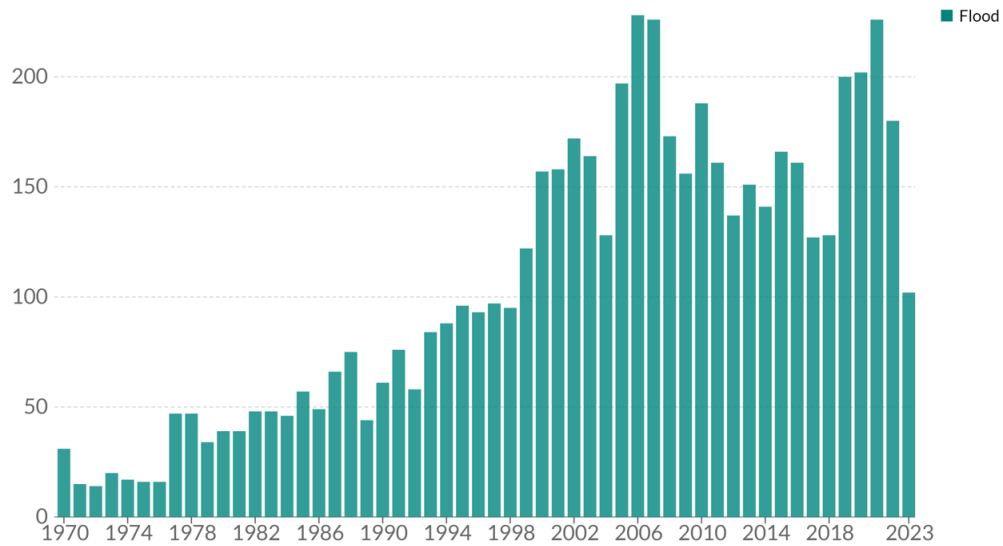


Imagen 5. – Global report of natural disasters by type between 1970 and 2023. Source: EM-DAT, CRED / UCLouvain (2023). <https://ourworldindata.org/natural-disasters>

On the other hand, the dynamics of the oil industry worldwide have been marked by the occupation of different geographical areas through the concession and exploitation of blocks or production fields, some of which are located in areas susceptible to floods. As a result, various hydrocarbon operational facilities (wells, production lines, pipelines, stations, refineries, etc.) are under some level of risk regarding these natural phenomena.

For example, in Colombia, a country particularly exposed to increases in precipitation due to the occurrence of meso and macro-scale climatic phenomena, such as La Niña, which result in extreme hydrological events such as floods (IDEAM, 2011), combined with the oil-producing nature of the territory, conditions are created for the occurrence of NaTech-type events. Among other resulting events, there is a high risk of incidents related to oil spills in aquatic and terrestrial environments, characterized by the absence of a methodological framework that allows for a predictive analysis of the behavior of the substance released into the environment and its effects on vulnerable receptors or elements (image no. 7).

In particular, the design and operation of equipment, processes, structures, and oil facilities follow a set of international industry standards and norms, which, in terms of safety, are proposed to withstand operational or internal process forces (temperature, pressure, flow rate, etc.), without considering the action of external forces (Cozzani et al., 2009), such as those exerted by the velocity (shear stresses) and depth of the water column during flooding events.

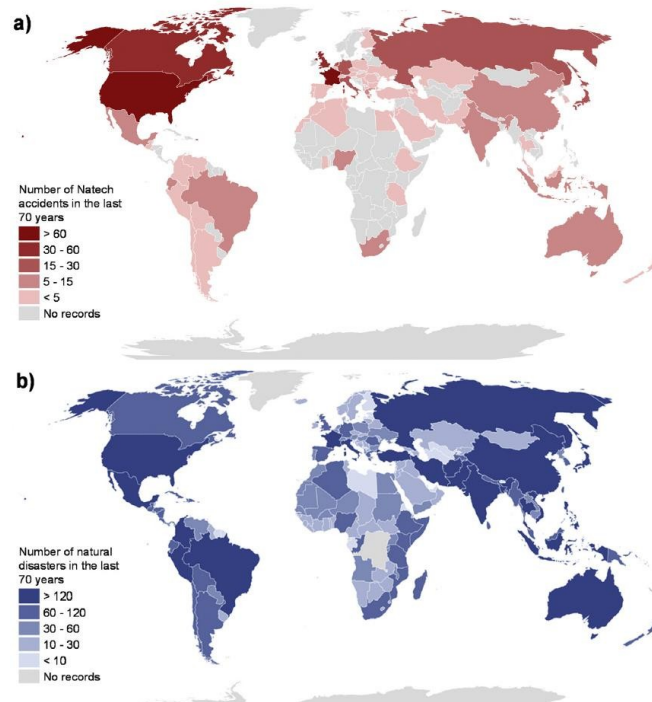


Image 6. Geographical distribution of NaTech events (a) recorded in databases and (b) geographical distribution of natural disasters recorded by the Centre for Research on the Epidemiology of Disasters (CRED, 2020) in the last 70 years.

In this sense, the absence of these safety barriers in the design, construction, and operation standards of equipment and processes constitutes a weakening condition of the facilities against natural threats and, therefore, opens the possibility of the occurrence of a NaTech-type event, whose domino effect can lead to Loss of Containment (LOC) of highly hazardous substances.

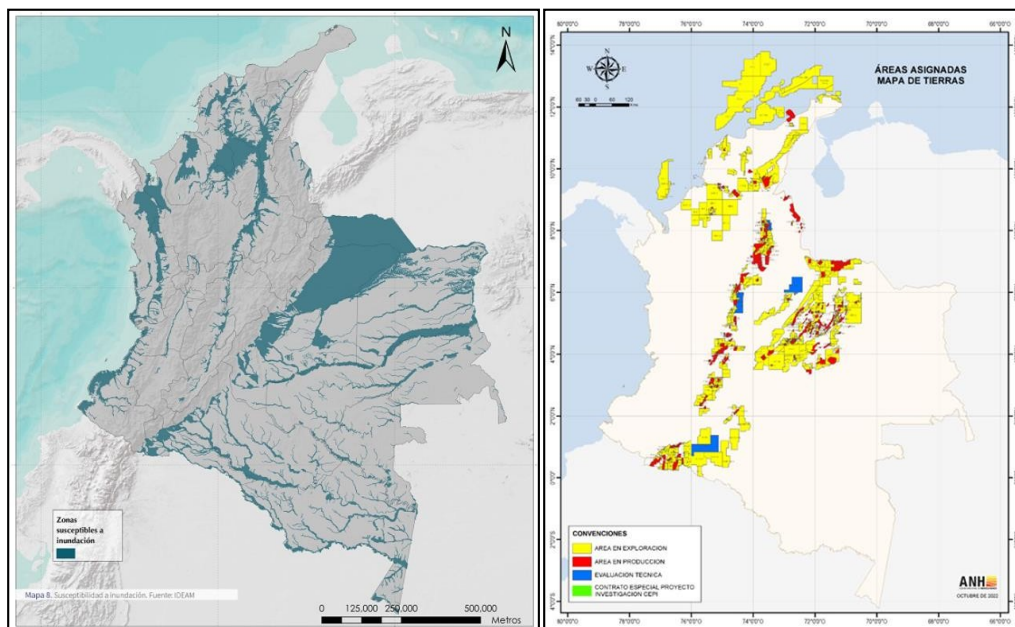


Image No. 7. – Left: Map of flood susceptibility in Colombia (2023). Source: IDEAM, 2023 - Right: Map of lands in areas assigned for the exploration and exploitation of hydrocarbons. Source: ANH, 2023

Misuri & Cozzani (2021), propose a risk assessment framework for NaTech events that not only considers a direct impact of the natural phenomenon on the equipment or process (image 8, a), but also, given the complexity of these events in relation to the level of damage, extent of the impacts, and multi-threat evolution or development of said phenomenon, the assessment framework can be panoramically broader, so that indirect pathways of impact are included (image 8, b). These pathways are characterized by damage or deterioration of the support and/or backup systems that allow for the proper functioning of equipment or processes, leading to the loss of containment of the hazardous substance.

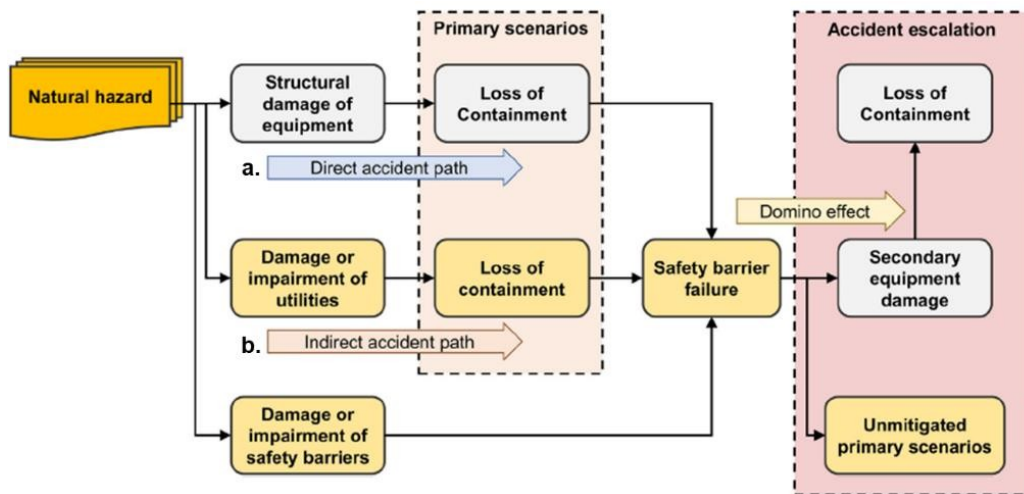


Image No. 8. –Evaluation of Natech events based on lessons learned from previous events related to the failure of auxiliary systems and safety barriers. Source: Cozzani & Misuri. 2021. A paradigm shift in the assessment of Natech scenarios in chemical and process facilities

2 NaTech Scenario Analysis: Hydrocarbon spills in storage tanks triggered by floods

Research conducted by Antonioni et al., 2009, Antonioni et al., 2015, regarding the quantitative risk assessment (QRA) for oil spills in storage tanks due to floods, propose analysis based on the characterization of the natural hazard and the vulnerability of the tanks. The latter is based on fragility models that determine the probability of damage to the equipment, while for the threatening phenomenon, they propose the analysis of the hydrological event, based on the external forces exerted by the depth of the water column and the velocity of the current, associated with a specific return period (Image 8), similar to what was evidenced by V. Cozzani et al., 2010, and V. Cozzani et al., 2014, regarding the relationship found between the depth of the flood and the occurrence of NaTech events (Image 9, right).

In this regard, the selection of the hydrological event as the starting point of the analysis will depend on the criteria established in the evaluation regarding the magnitude and probability of the flood of interest,

considering that the occurrence of these events is determined by a return period (t_r) in years whose frequency is estimated by (Antonioni et al., 2015):

$$f = \frac{1}{t_r}(1)$$

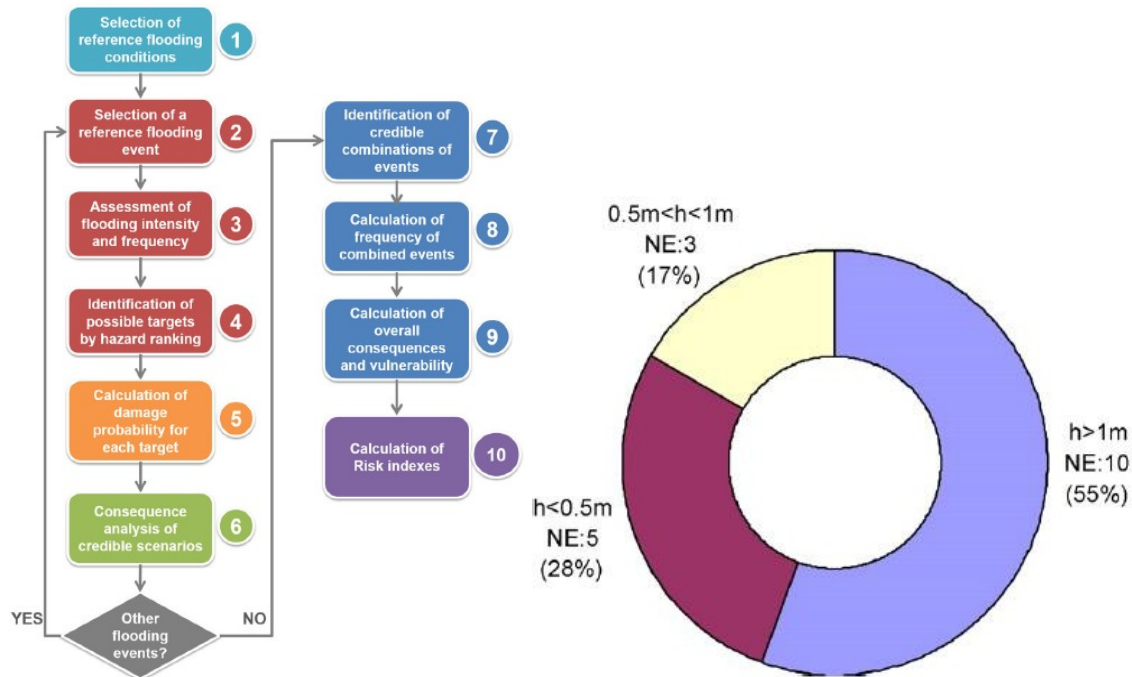


Image No. 9. – Left: Methodology for the quantitative risk assessment of NaTech scenarios triggered by extreme hydrological events. Source: Antonioni et al., 2015 - Right: Classification of 18 NaTech events caused by floods based on the maximum water height (h : maximum water height, m; NE: number of events). Source: V. Cozzani et al., 2010

From there, using hydraulic simulation methods, depths (hw) and velocities (vw) of the flood plume affecting the equipment under analysis (storage tank) are obtained. It is worth noting that through these two variables, the hydraulic effects associated with external forces exerted by slow submergence, deep-sea waves, moderate-speed waves, high-speed waves, and finally high-speed waves with limited depth are simplified (V. Cozzani et al., 2014).

Subsequently, it is necessary to determine the type and level of damage caused to the exposed equipment due to the flood. For this, various authors have proposed mechanical failure models that allow for estimating with some approximation the vulnerability of the equipment, including Salzano et al., 2003, G. Antonioni et al., 2009, G. Landucci et al., 2012, and G. Antonioni et al., 2015, whose contributions are represented by fragility curves (Image 10 and Image 11), mechanical failure models under flood load ((2) to (8)), and Table 1.

Once the vulnerability model of the equipment to the extreme hydrological event is determined, the failure mode that generates the consequence of interest is established. For this, V. Cozzani et al., 2010, propose based on the event tree (Image 3), three (3) failure modes in the tank due to the external forces exerted by the flood: R1 - Instantaneous leakage of the entire tank; R2 - Continuous leakage of the entire tank contents over a period, due to the catastrophic rupture of the largest diameter connection or structural failures.

R3 - Minor leaks or discharges due to partial ruptures in the tank connections or catastrophic ruptures of smaller diameter connections, while Antonioni et al., 2015, propose a catastrophic failure that triggers an instantaneous leakage of the entire container.

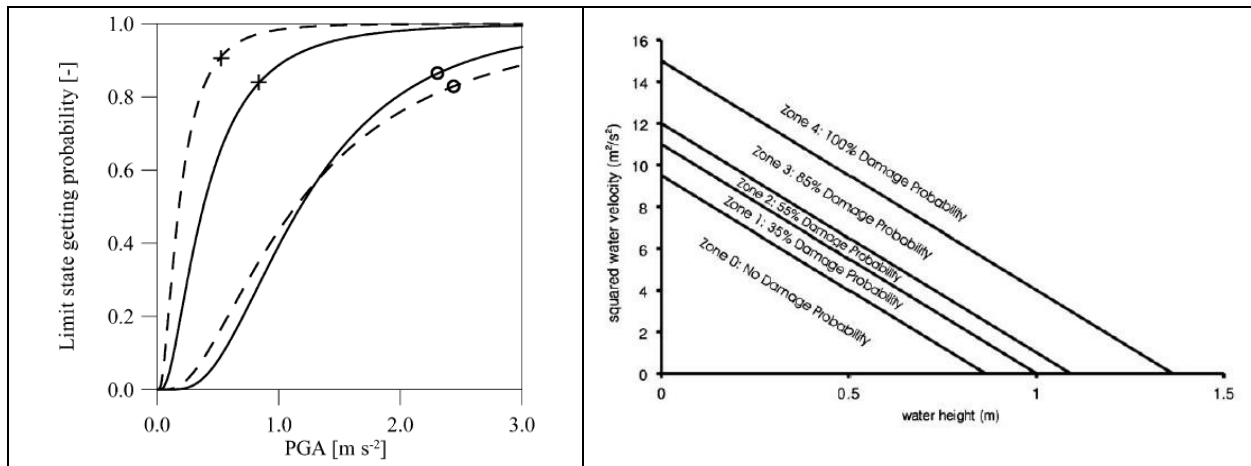


Image No. 10. – Fragility curves calculated for atmospheric steel tanks affected by earthquakes. Source: Salzano et al., 2003

Image No. 11. – Estimation of the probability of equipment damage with respect to the maximum water height (h) and the square of the maximum water velocity (V2). Source: Antonioni et al., 2009

$$P_w = P_{ws} + P_{wd} \quad (2)$$

$$P_w = P_{ws} + P_{wd} \quad (3)$$

$$P_{ws} = \rho_w g h_w \quad (4)$$

$$P_{wd} = \frac{1}{2} \rho_w k_w v_w^2 \quad (5)$$

$$P_{net} = P_{ws} + P_{wd} - P_f \quad (6)$$

$$P_f = \rho_f g H \phi \quad (7)$$

$$P_{net} \geq P_{cr} \quad (8)$$

$$P_{ws} + P_{wd} - P_f \geq P_{cr} \Rightarrow P_{ws} + P_{wd} \geq P_{cr} + P_f \Rightarrow P_w \geq P_{cr} + P_f$$

Donde:

- P_w : Flood load
- P_{ws} : Hydrostatic load exerted by the water column
- P_{wd} : Load associated with the kinetic energy of the water
- g : Gravity constant
- h_w : Water depth.
- ρ_w : Water density
- k_w : Hydrodynamic coefficient
- v_w : Water velocity
- P_r : Internal pressure of the tank
- p_f : Density of the fluid contained in the tank
-
- H : Tank height
- Φ : Nivel de llenado del tanque.
- P_{net} : Presión neta sobre el tanque.
- P_{cr} : Presión crítica

Equations of the failure mechanical model proposed by Salzano et al., 2003. - Source: Salzano et al., 2003

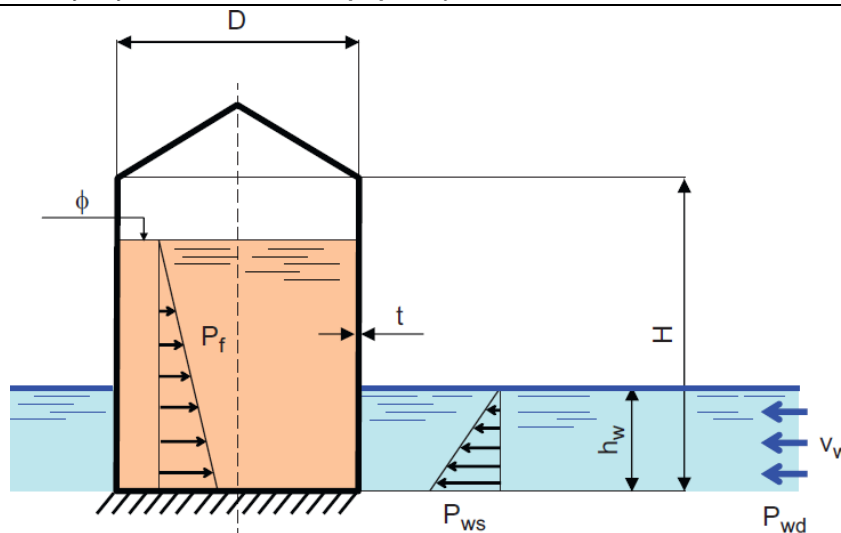


Image 12.. Schematic of the forces acting on flooded vertical atmospheric tanks.

Fuente: Salzano et al., 2003

Item	Definition	Value/Equation
Vulnerability model equations		
CFL_v	Critical Filling Level for vertical atmospheric vessels	$CFL_v = \left(\frac{C_{cr} \rho_w v_w^2}{2} + \rho_w g h_w - P_{cr} \right) / \rho_f g H$
P_{cr}	Vessel critical pressure (Pa) evaluated with the proposed simplified correlation	$P_{cr} = J_1 C + J_2$ in which $J_1 = -0.199$ $J_2 = 6950$
ψ	Vessel vulnerability due to flooding	$\psi = (CFL - \phi_{min}) / (\phi_{max} - \phi_{min})$
Input parameters		
C	Vessel capacity	Small capacity $C < 5000 \text{ m}^3$ Medium capacity $5000\text{--}10000 \text{ m}^3$ Large capacity $> 10000 \text{ m}^3$
v_w	Flood water speed ^a	0–3.5 m/s
h_w	Flood water depth ^a	0–4 m
ρ_w	Flood water density	1100 kg/m ³
ρ_f	Stored liquid density	650–1300 kg/m ³
K_w	Hydrodynamic coefficient	1.8
H	Vessel height	Small capacity 3.6–18 m Medium capacity 3.6–16.2 m Large capacity 3.6–7.2 m
g	Gravity acceleration	9.81 m/s ²
ϕ_{min}	Minimum operative filling level	0.01
ϕ_{max}	Maximum operative filling level	0.75

Table 1. Vulnerability model and input parameters for cylindrical atmospheric tanks involved in flood events. CFL: Critical fill level. Source: Antonioni et al., 2015

On the other hand, Rojas, S., 2005, Guerrero, Y., 2007, and Zapata C. et al., 2002, have evaluated various computational applications to predictively analyze the behavior of hydrocarbon spills in aquatic environments, mainly in continental waters in Colombia, in order to dimension the potential consequences, using different Lagrangian-type modeling software that converge in the calculation of the wear or weathering processes of the spill and the effects of hydrodynamics on the spill transport, with common estimates including advection, trajectory, destination, and losses due to evaporation, mechanical dispersion, adherence to shores or land borders, and dissolution, in models with different capabilities and types of licenses.



Image No. 13. – Oil spill formed after flood damage to storage tanks in Coffeyville, USA, in 2007. Source: Necci, Amos & Wood, Maureen & Krausmann, Elisabeth & Girgin, Serkan. (2020). Natech risk management Common Inspections Criteria.

The most commonly used mathematical formulations in the analysis of spill behavior in aquatic environments are shown in the following table:

Proceso	Formulación												
Transport (Discrete Lagrangian Algorithm)	$\vec{V}_t = \vec{V} + \vec{V}'$ Where: <ul style="list-style-type: none"> • \vec{V}_t: Drift velocity. • \vec{V}: Mean surface velocity due to the combination of wind and current effects. • \vec{V}': Turbulent fluctuation - Horizontal dispersion of oil spill 												
Hydrodynamics of the current	<ul style="list-style-type: none"> • Continuity Equation $\frac{\partial Q}{\partial x} + \frac{\partial A}{\partial t} = 0$ • Momentum Equation $\frac{\partial Q}{\partial t} + \frac{\partial \left(\frac{Q^2}{A} \right)}{\partial x} + gA \left(\frac{\partial y}{\partial x} - S_0 \right) + gAS_f = 0$ Where: <ul style="list-style-type: none"> • x: Distance in meters of the section to be evaluated. • t: Time in seconds • A: Cross-sectional area • y: Water depth. • S_0: Riverbed slope. • S_f: Energy gradient slope. • g: Acceleration due to gravity. 												
Advection	$\vec{V} = \alpha_w \vec{V}_w + \alpha_c \vec{V}_c$ Where: <ul style="list-style-type: none"> • \vec{V}_w: Drift velocity due to advection. • \vec{V}_w: Wind speed at ten meters above the water surface. • \vec{V}_c: Mean current speed relative to its depth. • α_w: Wind thrust factor on the spilled oil layer. • α_c: Thrust factor moving the oil layer due to the mean current speed. 												
Mechanical dispersion	<p>Table. Dispersion law for oil spills (Fay, 1971, Hoult, 1979, and Walkman et al., 1973)</p> <table border="1" data-bbox="581 1577 1279 1776"> <thead> <tr> <th>Fase de Dispersión</th> <th>Ancho, Le</th> <th>Radio, Re</th> </tr> </thead> <tbody> <tr> <td>Gravedad-Inercia</td> <td>$1.39(\Delta g A t^2)^{1/3}$</td> <td>$1.14(\Delta g V t^2)^{1/4}$</td> </tr> <tr> <td>Gravedad-Viscosidad</td> <td>$1.39(\Delta g A^2 t^{1/2} \nu^{-1/2})^{1/4}$</td> <td>$0.98(\Delta g V^2 t^{1/2} \nu^{-1/2})^{1/6}$</td> </tr> <tr> <td>Tensión Superficial-Viscosidad</td> <td>$1.43(\sigma^2 t^3 \rho_w^{-2} \nu^{-1})^{1/4}$</td> <td>$1.60(\sigma^2 t^3 \rho_w^{-2} \nu^{-1})^{1/4}$</td> </tr> </tbody> </table> <p>Nota: $A=0.5$ volumen del crudo/longitud del derrame. V= Volumen del derrame de crudo. $\Delta = 1 - (\rho_o/\rho_w)$. ν = viscosidad cinemática del agua.</p>	Fase de Dispersión	Ancho, Le	Radio, Re	Gravedad-Inercia	$1.39(\Delta g A t^2)^{1/3}$	$1.14(\Delta g V t^2)^{1/4}$	Gravedad-Viscosidad	$1.39(\Delta g A^2 t^{1/2} \nu^{-1/2})^{1/4}$	$0.98(\Delta g V^2 t^{1/2} \nu^{-1/2})^{1/6}$	Tensión Superficial-Viscosidad	$1.43(\sigma^2 t^3 \rho_w^{-2} \nu^{-1})^{1/4}$	$1.60(\sigma^2 t^3 \rho_w^{-2} \nu^{-1})^{1/4}$
Fase de Dispersión	Ancho, Le	Radio, Re											
Gravedad-Inercia	$1.39(\Delta g A t^2)^{1/3}$	$1.14(\Delta g V t^2)^{1/4}$											
Gravedad-Viscosidad	$1.39(\Delta g A^2 t^{1/2} \nu^{-1/2})^{1/4}$	$0.98(\Delta g V^2 t^{1/2} \nu^{-1/2})^{1/6}$											
Tensión Superficial-Viscosidad	$1.43(\sigma^2 t^3 \rho_w^{-2} \nu^{-1})^{1/4}$	$1.60(\sigma^2 t^3 \rho_w^{-2} \nu^{-1})^{1/4}$											
Adherence to shores	$V_2 = V_1 e^{-k(t_2-t_1)}$												

Proceso	Formulación																								
	<p>Donde:</p> <ul style="list-style-type: none"> • V_1 y V_2: Volumes of crude oil at the border over time t_1 y t_2. <ul style="list-style-type: none"> • $k: \frac{[-\ln(1/2)]}{\lambda}$ y λ is the half-life determined by the following table: <p>Table. Description of riverbanks and their parameters (Torgrimson, 1980)</p> <table border="1" data-bbox="764 506 1130 869"> <thead> <tr> <th>DESCRIPCION DE LA RIBERA</th> <th>VIDA MEDIA</th> </tr> </thead> <tbody> <tr> <td>Cabo o Promontorio</td> <td>1 hr</td> </tr> <tr> <td>Plataforma anti-oleaje</td> <td>1 hr</td> </tr> <tr> <td>POCKET BEACH</td> <td>1 día</td> </tr> <tr> <td>Playa de Arena</td> <td>1 día</td> </tr> <tr> <td>Playa de Arena y Grava</td> <td>1 día</td> </tr> <tr> <td>Playa de Arena y Guijarro</td> <td>1 año</td> </tr> <tr> <td>EXPOSED TIDE FLATS</td> <td>1 hr</td> </tr> <tr> <td>Ribera de roca protegida</td> <td>1 año</td> </tr> <tr> <td>SHELTERED TIDE FALT</td> <td>1 año</td> </tr> <tr> <td>Humedal Protegido</td> <td>1 año</td> </tr> <tr> <td>Tierra</td> <td>1 año</td> </tr> </tbody> </table>	DESCRIPCION DE LA RIBERA	VIDA MEDIA	Cabo o Promontorio	1 hr	Plataforma anti-oleaje	1 hr	POCKET BEACH	1 día	Playa de Arena	1 día	Playa de Arena y Grava	1 día	Playa de Arena y Guijarro	1 año	EXPOSED TIDE FLATS	1 hr	Ribera de roca protegida	1 año	SHELTERED TIDE FALT	1 año	Humedal Protegido	1 año	Tierra	1 año
DESCRIPCION DE LA RIBERA	VIDA MEDIA																								
Cabo o Promontorio	1 hr																								
Plataforma anti-oleaje	1 hr																								
POCKET BEACH	1 día																								
Playa de Arena	1 día																								
Playa de Arena y Grava	1 día																								
Playa de Arena y Guijarro	1 año																								
EXPOSED TIDE FLATS	1 hr																								
Ribera de roca protegida	1 año																								
SHELTERED TIDE FALT	1 año																								
Humedal Protegido	1 año																								
Tierra	1 año																								
<p>Evaporation</p>	$F = \left(\frac{1}{C} \right) \left[\ln P_0 + \ln \left(CK_E t + \frac{1}{P_0} \right) \right]$ <p>Where:</p> <ul style="list-style-type: none"> • t: It's the elapsed time. • C: It's an evaporation constant defined by the following equation: $C = 1158.9 API^{-1.1435}$ <p>Where: API it's the specific gravity of the crude oil under the following relationship:</p> $API = \frac{141.5}{SG} - 131.5$ <p>Where: SG it's the value of the typical molar volumen for petroleum fuels, wich is $200 \cdot 10^{-6} \text{ m}^3/\text{mol}$.</p> <ul style="list-style-type: none"> • K_E: It's the exponent of evaporation defined by: $K_E = \frac{0.0025U^{0.7} Av}{RTV_0}$ <p>Where:</p> <ul style="list-style-type: none"> • U: It's the wind speed measured at ten meters above sea level. • A: Spill area. • R: Ideal Gas constant. • T: oil Temperature. • v: Molar Volume. <p>Additionally:</p> <ul style="list-style-type: none"> • P_0: Initial vapor pressure in atmospheres at TE, that is, at surface temperature, which is defined as: $\ln P_0 = 10.6 \left(1 - \frac{T_o}{T_E} \right)$ <p>Where:</p> <ul style="list-style-type: none"> • T_o: It is the reference or boiling temperature of the crude defined by: 																								

Proceso	Formulación															
	$T_o = 542.6 - 30.275 API + 1.565 API^2 - 0.03439 API^3 + 0.0002604 API^4$															
Emulsification	$\frac{dF_{wc}}{dt} = K_{wc} (U_{10} + 1)^2 \left[\frac{1 - F_{wc}}{OC_1} \right]$ <p>Donde:</p> <ul style="list-style-type: none"> • F_{wc}: Water fraction in oil • K_{wc}: Emulsification coefficient of 2×10^{-6} for light oil or 4.5×10^{-6} for heavy oils. • U_{10}: Wind speed. • OC_1: it is 0.7 for light crude oil and 1.15 for heavy crude oil. 															
Dissolution and dispersion	$\frac{dm}{dt} = KA_s C_o e^{-\alpha}$ <p>Where:</p> <ul style="list-style-type: none"> • m: Oil slick mass. • K: Oil slick transfer coefficient. • A_s: Surface área of the slick. • α: Devcay exponent. • C_o: Solubility of oil in fresh water. <p>The Values of K, C_o y α were determined by Yapa (1994) for heavy an light crude oils as follows:</p> <p style="text-align: center;">Tabla. Constantes de disolución</p> <table border="1" style="margin-left: auto; margin-right: auto;"> <thead> <tr> <th>Tipo de Cruído</th> <th>C_o</th> <th>K</th> <th>KC_o</th> <th>α</th> </tr> </thead> <tbody> <tr> <td>Pesado</td> <td>7.88</td> <td>0.002335</td> <td>0.0184</td> <td>0.423</td> </tr> <tr> <td>Ligero</td> <td>21.3</td> <td>0.041502</td> <td>0.884</td> <td>2.380</td> </tr> </tbody> </table> <p style="text-align: center;"><small>Source: Yapa P. y Shen H. 1994. "Modelling River Oil Spill: A Review, Journal of Hydraulic Reserch."</small></p>	Tipo de Cruído	C_o	K	KC_o	α	Pesado	7.88	0.002335	0.0184	0.423	Ligero	21.3	0.041502	0.884	2.380
Tipo de Cruído	C_o	K	KC_o	α												
Pesado	7.88	0.002335	0.0184	0.423												
Ligero	21.3	0.041502	0.884	2.380												
Viscosity corrections	<p>By water content:</p> $\mu = \mu_o \exp \left[\frac{2.5 F_{wc}}{1 - 0.65 F_{wc}} \right]$ <p>Donde:</p> <ul style="list-style-type: none"> • μ_o: It's the initial viscosity of the oil • F_{wc}: Water content. <p>By evaporation:</p> $\mu = \mu_o \exp [C_2 * F_{evap}]$ <p>Where:</p> <ul style="list-style-type: none"> • F_{evap}: Evaporated fraction of the spill • C_2: Varies between 1 and 10, with 1 for light fuels. <p>By Temperature:</p> $\mu = \mu_o \exp [8770 T_K^{-1} - 29.4]$ <p>Where:</p> <ul style="list-style-type: none"> • T_K Ambient temperature. 															
Corrections density	$\rho = F_W \rho + (1 - F_{evap}) \rho_o$ <p>Where:</p> <ul style="list-style-type: none"> • F_{evap}: Evaporated fraction of the spill 															

Proceso	Formulación
	<ul style="list-style-type: none"> • F_w: Water content. • ρ_o: Density of the Oil. • ρ: Density of water.
<i>Table 2. Formulations used in the analysis of hydrocarbon spill behavior in rivers Source: Zapata C. et al., 2002</i>	

On the other hand, in an effort to estimate the behavior of hydrocarbon fires that occur during a spill, Imazu & Nishino (2018) propose considering such a spill as a set of circular particles that float while burning, whose temporal positions depend on the velocity field and trajectories of the flood, and whose initial ignition is unpredictable. The combustion zone and the radiant heat flux for each of the burning particles are estimated homogeneously and independently of the wind direction, from the center of the hydrocarbon particle, and ceases when the thickness of each spill particle reaches 1 mm.

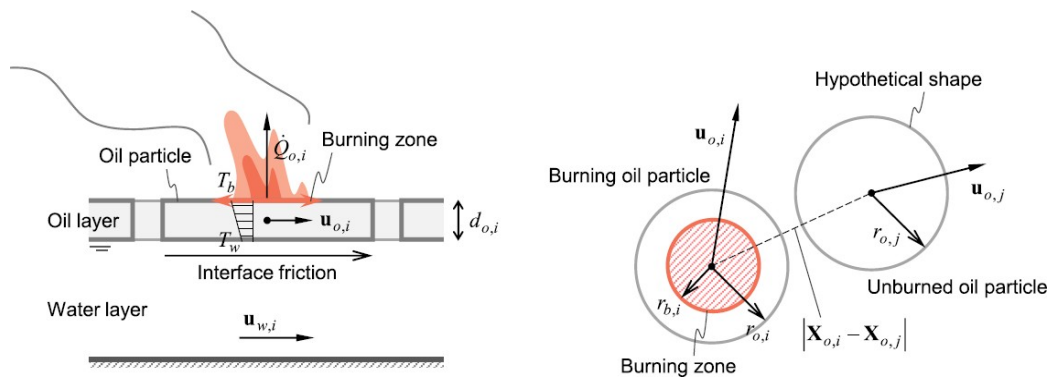


Image 14. Scheme of a fire spread model due to a hydrocarbon spill. Source: T. Nishino, Y. Imazu, 2018.

2.1 Treatment of NaTech Risk with Process Safety Approach

The layers of protection applicable to equipment and processes exposed to external forces exerted by natural phenomena, according to the concept proposed by CCPS (2001), as safety barriers, provide technical solutions to avoid, prevent, or mitigate containment losses within a wide spectrum of alternatives ranging from passive barriers to active ones.

Lessons learned from NaTech events worldwide, as gathered by Misuri et al. (2019) and various authors, highlight common failures in safety barriers, including water supply shortages for fire protection systems (Steinberg & Cruz, 2004), unavailable water and foam vapor suppression systems (Girgin, 2011), clogged spill containment systems (eMars), unavailable cooling chemical storage (Additives for Polymers, 2017), flooded and inaccessible manual valves (NTSB, 1996), and completely flooded backup power generators (Labib and Harris, 2015), among others.

According to Necci A., Krausmann E. (2021), some examples to address the risk associated with natural threats can range from physical barriers such as: construction of dikes, construction of artificial channels, stabilization of riverbanks, compaction and stabilization of soils, reorganization of industrial facilities, and proper plant location, while in terms of procedural measures, the definition of roles and functions, as well as the list of actions and response times, will contribute to risk reduction.

According to Necci A., Krausmann E. (2021), some examples of dealing with the risk associated with natural threats can range from physical barriers such as: construction of dikes, construction of artificial channels, stabilization of riverbanks, compaction and stabilization of soils, reorganization of industrial facilities, and proper plant location, while in terms of procedural measures, defining roles and functions, as well as listing actions and response times, will contribute to risk reduction.

In a NaTech scenario related to the impact on crude oil storage tanks due to extreme hydrological events, it is crucial to focus on process safety and identify the risks associated with the threatening event and its evolution. Here are some specific aspects that could be included as risk treatment measures:

Regarding the threatening phenomenon:

- Installation and monitoring of multi-criteria early warning systems, allowing real-time assessment of triggering rain pulses and the levels and flow velocity in the threatening stream.
- Analyze and characterize hydrologically and hydrodynamically the behavior of the stream under extreme climatic scenarios, so that the flood extent, flow velocities, impacted areas by the flood, and potentially exposed equipment to the hydrological phenomenon can be identified.
- Periodically monitor changes in the fluvial morphodynamics of the stream, identifying erosion and/or sedimentation processes that could lead to changes in the flow path and potential increase in risk level.

Regarding the exposed equipment and process:

- Perform process hazard analysis (PHA) involving quantitative risk analysis (QRA), to identify the different final events or consequences (effects) associated with the individual failure of the vessel and under a domino effect.
- Inherently safe design of the tank, considering resistance to external forces exerted by the threatening natural phenomenon.
- Identification of equipment and/or units complementary to the vessel that could be affected by flooding.
- Installation of anchoring mechanisms in the tank and complementary or attached units.

- Sizing of fixed spill containment systems such as dikes, skimmers, and perimeter drains.
- Based on the results of the hydrological and hydrodynamic modeling of the flood, construct containment walls to partially or fully retain the inundation.
- Design and implementation of shutdown or process cutoff mechanisms.
- Design and implementation of procedures and mechanisms for draining and/or transferring inventories stored in exposed tanks.
- Design, construction, and maintenance of industrial facility stormwater drainage systems.

Regarding emergency management:

- Updating emergency plans, considering NaTech risk scenarios.
- Based on the consequence modeling of the event, dimension the response capacity (resources) to address NaTech risk scenarios.
- Update or incorporate response procedures and strategies for managing emergencies originating from NaTech events.
- Design internal response strategies that can be articulated with the external response strategies of state or governmental entities at the local, regional, and national levels.
- Establishment of an emergency management escalation procedure, from operational to crisis and business continuity levels.
- Design and development of training programs for internal and external response teams in managing NaTech events.
- Design and execution of a program of drills and simulations with internal and external response teams in managing NaTech events.

2.2 Case Study

In order to evaluate the methodological approaches proposed by the various authors related in section 2 of this document, the behavior of a hypothetical NaTech event in an industrial facility that receives, processes, treats, and dispatches wet gas, located in the floodplain of a high-flow river, has been analyzed.

Inputs to understand the behavior of an extreme hydrological phenomenon in the study area included the collection of topographic information using LiDAR (Light Detection and Ranging or Laser Imaging Detection and Ranging) technology captured through the use of an unmanned aerial vehicle (drone) with RTK technology (image 15), which allowed the collection of altitudinal and morphometric data from the floodplain, the watercourse (bathymetrically corrected), and the plant surface (digital surface model) (image 15a, b, and c), with precision ranges of ± 0.1 m, as detailed in Table 3.

² ESRI. Disponible en: <https://desktop.arcgis.com/es/arcmap/latest/manage-data/las-dataset/what-is-lidar-data-htm>

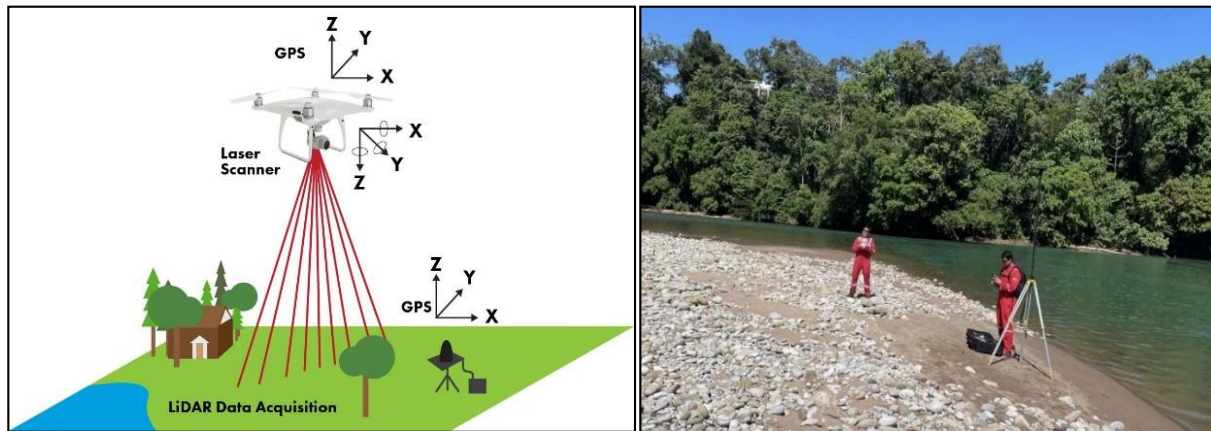


Image 15. Left. Illustrative diagram of LiDAR technology with drone. Source: FlyGuys. Available at: <https://flyguys.com/5-industry-use-cases-for-lidar/> Right. Topographic survey with LiDAR technology. Source: SACS Consultores, 2022.

Aeronave	
Manufacturer	<ul style="list-style-type: none"> • DJI
Series	<ul style="list-style-type: none"> • Phantom 4 RTK
Weight	<ul style="list-style-type: none"> • 1391 g.
Diagonal size	<ul style="list-style-type: none"> • 350 mm.
Maximum ascent speed	<ul style="list-style-type: none"> • 6 m/s
Maximum descent speed	<ul style="list-style-type: none"> • 3 m/s
Maximum speed	<ul style="list-style-type: none"> • 58 km/h
Maximum altitude range	<ul style="list-style-type: none"> • 6000 m.
Wind speed resistance limit	<ul style="list-style-type: none"> • 10 m/s.
Maximum flight duration	<ul style="list-style-type: none"> • 30 minutes approximately
Operating environmental temperature range	<ul style="list-style-type: none"> • 0°C a 40°C
Precision Range	<ul style="list-style-type: none"> • RTK Connected and functioning properly: Vertical: $\pm 0.1\text{m}$ - Horizontal: $\pm 0.1\text{m}$. • RTK disconnected: $\pm 0.1\text{m}$ with visual positioning- $\pm 0.5\text{m}$ with GNSS positioning. Horizontal: $\pm 0.3\text{m}$ with visual positioning - $\pm 1.5\text{m}$ with GNSS positioning.
GNSS	
Single frequency High-sensitivity GNSS	<ul style="list-style-type: none"> • GPS + BeiDou + Galileo (Asia); GPS +Glonass + Galileo (other regions)
Multifrequency - High-precision RTK-GNSS multi-system	<ul style="list-style-type: none"> • GPS L1/L2; Glonass: L1/L2; BeiDou B1/B2; Galileo E1/E5 • Adjustment time less than 50 seconds.

Aeronave	
	<ul style="list-style-type: none"> • Position accuracy: Vertical de 1.5 cm. + 1 ppm (RMS); Horizontal 1 cm + 1 ppm (RMS).
Cámara	
Sensor	<ul style="list-style-type: none"> • 1" CMOS; effective pixels: 20M
Lens	<ul style="list-style-type: none"> • FOV (Field of View) 84°, 8.8 mm (35 mm in equivalent format: 24 mm.) f/2.8 - f/11, autofocus de 1 m - ∞
ISO Range	<ul style="list-style-type: none"> • Video: 100 - 3200 (Auto), 100 - 6400 (Manual) • Foto: 100 - 3200 (Auto), 100 - 12800 (Manual)
Mechanical shutter	<ul style="list-style-type: none"> • 8 - 1/2000 s
Electronic shutter	<ul style="list-style-type: none"> • 8 - 1/8000 s
Maximum image size	<ul style="list-style-type: none"> • 4864x3648(4:3); 5472x3648(3:2)

Table 3. Aircraft an LIDAR data characteristics

On the other hand, the data corresponding to the hydrological estimation of the flood in the water body were obtained through statistical and probabilistic treatment techniques of flow time series to obtain the magnitudes of said event with a return period (T_r) of 100 years, which, in terms of frequency, corresponds to an event with a probability of occurrence of 0.01.

Once the magnitude of the threatening event was estimated based on its probability of occurrence, a computational modeling approach based on the finite volume method was employed to understand hydraulically the behavior of the flood in the channel and floodplain where the gas plant is located. This was achieved by creating a computational domain with a modeling geometry that allowed refining the hydraulic calculation mesh into a network of triangles with accuracies of up to 1 m. The set of Navier-Stokes equations was developed, ensuring the principle of mass conservation throughout the mesh of that domain.

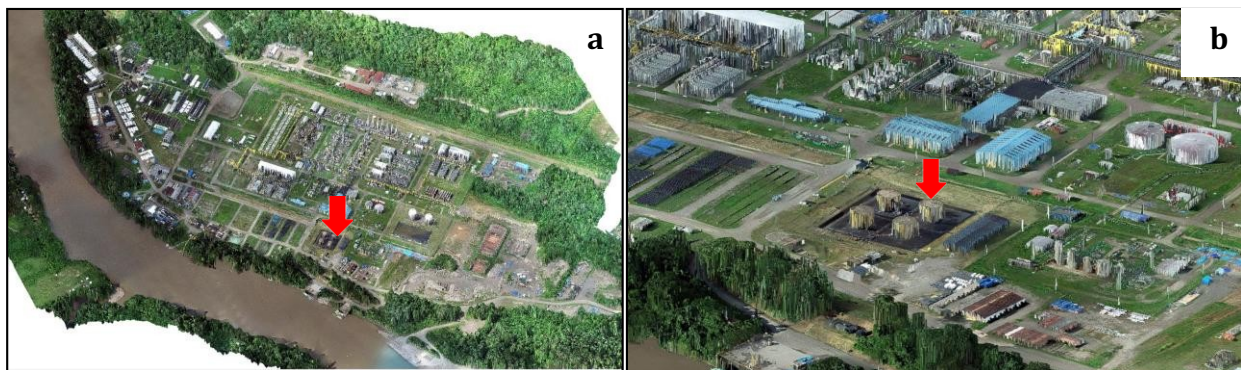




Image 16. a. Orthogonal photogrammetry of the gas plant. b. Digital surface modeling + Photogrammetry of the gas plant. c. Digital surface model of the gas plant. Note: In red arrow, affected storage tank. Source: SACS Consultores, 2022.

As a result of the simulation, the velocity and depth fields of the flood were obtained, which, according to the findings of V. Cozzani et al. (2010) in the accident records of flooding in storage tanks and based on the approach by Salzano et al., 2003 regarding the forces experienced by such equipment during a hydrological event, meet the conditions of water velocities greater than 1 m/s (image 17, left) and flood depths greater than 1 m (image 17, right), which would imply an impact on the existing refined hydrocarbon storage tanks within the installation, the subject of this analysis.

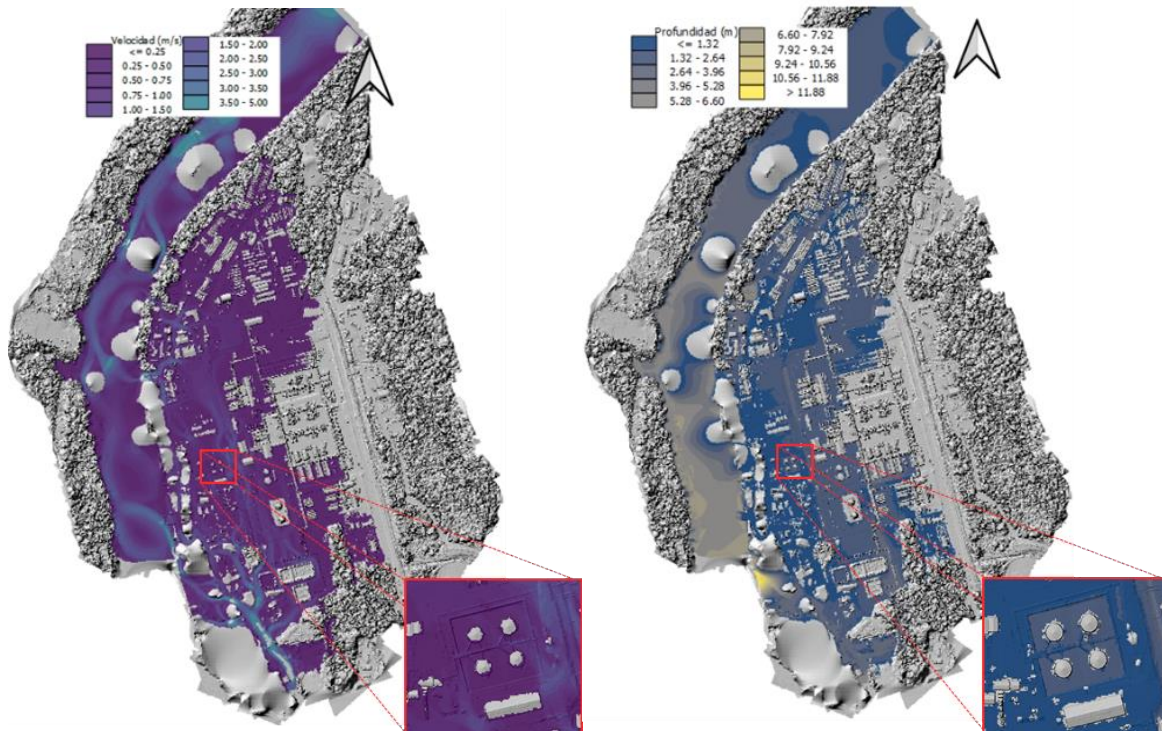


Image 17. Left: Raster of flood velocities in the channel, floodplain, and interior of the gas plant (Zoom on tank cluster). Image 16. Right: Raster of flood depths in the channel, floodplain, and interior of the gas plant (Zoom on tank cluster). Source: SACS Consultores, 2022.

The data corresponding to the hydrocarbon storage tanks (dimensions and volume), as well as the characteristics of the spilled product and the resulting balance of forces between the thrust force and the counteracting force exerted by the tank and its contents, are shown in Table 4.

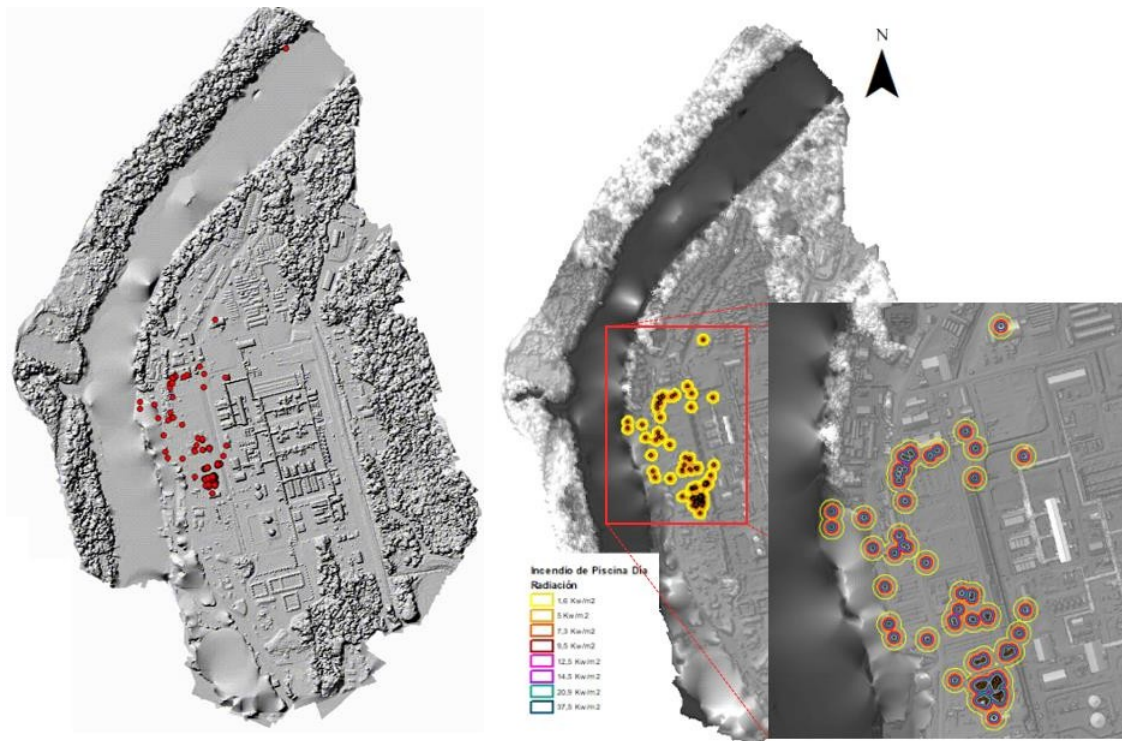


Image 18. Left: Trajectory of the hydrocarbon spill - Red particles. Right: Fire pools generated by the ignition of the hydrocarbon spill. Source: SACS Consultores, 2022.

Dato	Valor
Tank tipe	Atmospheric - Vertical
Tank height (m)	12.1
Tank diameter (m)	10
Tank material	Acero
Steel elasticity modulus (Pa)	2.1×10^{11}
Tank capacity (bbl.)	6000 aprox.
Product	Diesel
Diesel density (kg/m3)	850
Dike height (m)	0.8
Water density (kg/m3)	≈ 1000
Water velocity (m/s)	1.5
Water depth (m)	2
Hydrodynamic coefficient of the flood (adim.)	1.8
Hydrological event frequency (Year-1)	1×10^{-2}
Hydrodynamic pressure of the flood (P _{wd}) (Pas)*	19620
Hydrostatic pressure of the flood (P _{ws}) (Pas)*	3600
Total pressure exerted by the flood (P _{wd} + P _{ws}) (Pas)*	23220

Dato	Valor
Tank filling pressure (Counteracting) (Pf) (Pas)*	15134
Φ operational tank filling level factor*	0.15
Critical tank pressure (Pcr) (Pas)*	6760
Tank resistance pressure (Pcr + Pf)*	21894
Tank failure type	Buckling
Hydrocarbon spill volume (bbl.)	900

Table 4. Summary of input data applied in the present study - *Obtained by applying Landucci et al., 2012

The modeling result shows that, after the first hour of the event, the hydrocarbon spill is mostly contained within the gas plant (image 18, left), while a small portion of the spill reaches the nearby body of water. Regarding the adopted fire pool model (applying Imazu & Nishino, 2018 & Det Norske Veritas (DNV), 2009), it is observed that the fire puddles reach several critical equipment or process units of the installation (image 18, right), whose potential consequences could lead to a domino effect or escalation of the emergency.

2.3 Conclusions

The occurrence of natural phenomena, as the years go by, shows an increasing trend not only in their frequency but also in their magnitude or severity, covering larger areas that, as industrialization progresses, are occupied by facilities that receive, process, store, and dispatch hazardous substances to public health and the environment.

In that line of thought, the exposure of equipment or process units is becoming increasingly frequent, and efforts from regulatory authorities to risk owners seem not to be robust and rigorous enough to establish effective barriers and controls to address NaTech events.

Aspects such as natural climate variability associated with the ENSO phenomenon (in some regions) or induced variability, such as the effect of climate change, have shown a close correlation with the manifestation of more severe and intense natural phenomena. This implies that industrial projects or assets will necessarily have to incorporate these types of trend scenarios within the installation's risk landscape.

Various investigations published by different authors show approaches to determine the type of damage and potential consequence of a simplified event on an exposed equipment, or the potential damage triggered simultaneously in a complex domino-type event, considering the initiating event (flood, lightning storm, earthquakes, etc.), the geometry and structure of the exposed equipment, and finally, the type of substance contained.

In this sense, computational tools to understand the magnitude of the impact triggered by a loss of containment play a crucial role in sizing both the risk scenario and the emergency scenario. This will allow organizations to reduce uncertainty regarding the event's behavior and prepare to act, mitigating the impact of NaTech events on the facility and its surroundings.

From the risk management perspective with a focus on process safety management, aspects such as the implementation of Early Warning Systems (EWS) to detect the occurrence of natural phenomena that could potentially trigger a technological accident early on are vital for treating and reducing the installation's risk. Structural and organizational measures, such as the construction of dikes and the adoption of an emergency plan, respectively, will significantly contribute to mitigating the impacts and effects of NaTech events.

3 References and Bibliography.

3.1 Bibliography

- Antonioni, G., Bonvicini, S., Spadoni G., Cozzani, V. (2009). *Development of a framework for the risk assessment of Na-Tech accidental events*. Journal Reliability Engineering and System Safety 94 (2009) 1442–1450.
- Antonioni, G., Landucci, G., Necci, A., Gheorghiu, D., Cozzani, V. (2015). *Quantitative assessment of risk due to NaTech scenarios caused by floods*. Journal Reliability Engineering and System Safety 142 (2015) 334 – 345.
- Cozzani, V., Campedel, M., Renni, E., Krausmann, E. (2010). *Industrial accidents triggered by flood events: Analysis of past accidents*. Journal of Hazardous Materials 175 (2010) 501–509.
- Di Maio, F., Tonicello P., Zio E. (2022). *Modeling and Analysis Framework for Integrated Energy Systems Exposed to Climate Change-Induced NaTech Accidental Scenarios*. Sustainability 2022, 14, 786.
- Jiang, P., Tong, S., Wang, Y., Xu, G. (2021). *Modelling the oil spill transport in inland waterways based on experimental study*. Environmental Pollution 284 (2021) 117473.
- Jones, C., Sambanis, A., Kim, S., Cailas, M. (2020) *Chemical facility risks to natural flooding hazards in the United States*. Progress in Disaster Science 6 (2020) 100105
- Khakzad, N., Van Gelder, P. (2017). *Vulnerability of industrial plants to flood natechs: A Bayesian network approach*. Reliability Engineering and System Safety (2017), doi: 10.1016/j.ress.2017.09.016
- Landucci, G., Tugnoli, A., Antonioni, G., Cozzani, V. (2013). *Damage Models for Storage and Process Equipment Involved in Flooding Events*. Chemical Engineering Transactions, 31, 697-702 DOI: 10.3303/CET1331117.

- Landucci, G., Antonioni, G., Tugnoli, A., Cozzani, V. (2012). *Release of hazardous substances in flood events: Damage model for Atmospheric storage tanks*. Journal Reliability Engineering and System Safety 106 (2012) 200 – 216.
- Landucci, G., Necci, A., Tugnoli, A., Antonioni, G., Cozzani, V. (2014). *NaTech Scenarios Caused by Flooding: Evaluation of Accident Frequency by the Use of Fragility Models*. Chemical Engineering Transactions, 36, 427-432 DOI: 10.3303/CET1436072.
- Landucci, G., Necci, A., Tugnoli, A., Antonioni, G., Cozzani, V. (2014). *Release of hazardous substances in flood events: Damage model for horizontal cylindrical vessels*. Journal Reliability Engineering and System Safety 132 (2014) 125 – 145.
- Landucci, G., Antonioni, G., Necci, A., Cozzani, V. (2016). *Quantitative Risk Assessment of Cascading Events Triggered by Floods*. Chemical Engineering Transactions, 48, 901-906 DOI: 10.3303/CET1648151.
- Misuri, A., Landucci G., Vivarelli, S., Bonvicini, S., Cozzani, V. (2019). *Risk-based Vulnerability Analysis of Chemical Facilities Affected by Flooding*. Chemical Engineering Transactions, 77. DOI: 10.3303/CET1977088.
- Rojas, S. (2005). *Modelación de derrames de crudo en cauces – Aplicación al río Magdalena*. Tesis de grado. Facultad de ingeniería – Departamento de ingeniería civil y ambiental. Universidad de los Andes.
- Salzano, E., Iervolino, I., Fabbrocino, G. (2003). *Seismic risk of atmospheric storage tanks in the framework of quantitative risk analysis*. Journal of Loss Prevention in the Process Industries 16 (2003) 403–409.
- Yang Y., Chen G., Reniers G. (2019), *Vulnerability assessment of atmospheric storage tanks to floods based on logistic regression*. Journal Reliability Engineering and System Safety.
- Yapa, P., Shen, H., Angamma, K. (1993). *Modeling oil spills in a river-lake system*. Journal of Marine Systems 4 (1994) 453-471.
- Zapata, C., Calle, E., Parra, L. (2002). *Simulación del comportamiento fisicoquímico de derrames de hidrocarburos en ríos*. Escuela de geociencias y medio ambiente, Facultad de Minas. Universidad Nacional de Colombia Sede Medellín. *Avances en recursos hidráulicos 2002, Número 9* (pp. 7-18).
- Zuluaga, S., Sánchez M., Ramírez O., Muñoz F. (2019). *Development of parametric fragility curves for storage tanks: A Natech approach*. Journal Reliability Engineering and System Safety 189 (2019) 1 – 10.

3.2 *References*

Cruz, W. (2020). Explotador RPAS/Profesional GIS. SACS Group. Adquisición de información topográfica mediante sobrevuelos LiDAR.